THE DEVELOPMENT OF SEGMENTED HIGH RESOLUTION FAST NEUTRON SPECTROMETER

J. N. Abdurashitov[a]*, V. N. Gavrin[a], V. L. Matushko[a],
M. F. Mustafin[a], <u>A. A. Shikhin[a]†</u>, I. E. Veretenkin[a], V. E. Yants[a],
J. S. Nico[b], A. K. Thompson[b]

[a] Institute for Nuclear Research, Russian Academy of Sciences
Moscow, 117312, Russia
[b] National Institute of Standards and Technology
Gaithersburg, MD 20899 USA

Abstract

We present the development of a spectrometer based on full energy absorption using liquid scintillator doped with enriched ^{6}Li. Of specific interest, the spectrometer is expected to have good pulse height resolution, estimated to lie in the range (10–15)% for 14 MeV neutrons. It should be sensitive to fluence rates from 10^{-4} cm^{-2} s^{-1} to 10^2 cm^{-2} s^{-1} above a threshold of 500 keV in an uncorrelated γ-background of up to 10^2 s^{-1} ($E_\gamma > 100$ keV). The detector's efficiency is determined by the volume of the scintillator ($\sim$1.2 l) and is estimated to be (0.2–0.5)% for 3 MeV neutrons. The good pulse height resolution is achieved by compensation of the non-linear light-yield of the scintillator due to the use of optically separated segments, which collect scintillations from each recoil proton separately. We have constructed a pilot version of the detector using undoped liquid scintillator, and we demonstrate here the response of the detector to neutrons from a Pu-α-Be source, whose energies range up to 10 MeV and the response of the detector to 14.1 MeV neutrons from a D-T source also. Initial testing indicates a low threshold ($\approx$600 keV) and good spectral response after requiring a multiplicity of three segments. Such a spectrometer has applications for low-background experiments in fundamental physics research, characterizations of neutron fluence in space, and the health physics community.

1   Introduction

Because the neutron is a neutral particle, it does not produce direct ionization in matter, and thus one cannot measure its energy as one does with charged particles. Nevertheless, it can scatter on nuclei and transfer some part of initial energy to recoil particles.

---

*Corresponding author: jna@inr.ru

†e-mail: shikhin@inr.ru

Those recoils, however, do produce significant ionization and are able to ionize a detector medium. Therefore, in measuring the ionization of a medium irradiated with neutrons, one is able to estimate its initial energy. In organic media a neutron with an energy in the range of 1 MeV to 30 MeV loses its energy primarily through collisions with hydrogen. Due to the simple kinematics of elastic scattering, it is the most common medium for looking at recoil events. In recent decades, techniques based on full absorption of neutrons in organic scintillators that have been doped or mixed with an isotope with a large neutron capture cross section, such as ^{6}Li or ^{10}B, have undergone significant development [1, 2]. The detection of prompt scintillations from recoil protons in the medium followed by delayed neutron capture ensures that the energy released by the recoils corresponds to the full absorption of neutron. Such devices are referred to as capture gated fast neutron spectrometers.

The most significant obstacle to obtaining good energy resolution in such a detector is the poor pulse height resolution. The response to monoenergetic neutrons usually consists of two clearly distinguishable peaks [2]. Moreover, it reveals some of the dynamics. In particular, the relative intensities of the peaks change with the energy of incident neutrons. This behavior has been explained from the point of view of the multiplicity of recoil protons in combination with the nonlinear light-yield of the medium [3].

To illustrate the concept, consider the moderation of monoenergetic neutrons with an energy E_n in organic medium containing only hydrogen. Those neutrons transmit their energy to recoil protons E_{p_i} by elastic scattering. If a neutron was captured, the condition

$$E_n = \sum_i (E_{p_i})$$

is satisfied. Due to the kinematics in each collision, the neutron loses on average half of the energy that it had before the collision. The number of recoil protons, as well as distribution of their energy in each particular moderation event, differ in statistical weight and depend on E_n only. For example, 14.1 MeV neutrons decelerating to 0.5 MeV (the detection threshold) will produce recoil protons with a multiplicity distribution that is on average 4–5 recoils with FWHM ~100%.

Due to quenching effects, the specific light-yield in organic scintillators is not proportional to the energy of a recoil proton. Therefore, from the point of view of total light yield, the moderation process proceeds by two primary modes. In the first, multiple recoils occur and the total light yield depends strongly on the how the energy of each neutron was distributed among the recoil protons. The diffusion of the total light yield corresponds to a multiplicity distribution with a broad asymmetric peak. In the second mode, a neutron loses all (or almost all) its energy in a single collision. In this case the light is emitted by single recoil proton. The total light yield is unambiguous because the energy of that recoil is fixed; therefore, this mode of moderation will contribute to the pulse height response as a separate and relatively narrow peak. This peak always appears above the multiple one because in this mode the recoil proton has its highest energy.

Thus, capture-gated spectroscopy does not lend itself well to performing spectroscopy with good resolution. The relationship between the intensities of the two peaks corresponds to relative probability of two modes of moderation. One can understand the dynamics of the energy response also. For example, in a large detector all possible combinations of recoils and their energy will be realized. The multiplicity distribution will

be wide, and the contribution of a single recoil mode will be small. In a sufficiently small detector, the probability for neutron to lose all its energy in a single collision will increase significantly in comparison to that of moderation with multiple recoils, but the total probability for a neutron to be captured will decrease. If the neutron did not lose all its energy in the first collision, it will most probably leave detector medium, i.e., in a small detector there is little chance for the neutron to make a second collision before capture.

Monte-Carlo simulations of this process are consistent with the explanation, and we proposed a procedure for correcting the measurement of the total energy of a neutron [3]. It is necessary to measure amplitude of the scintillation from each recoil proton $I(E_{p_i})$. Although the light-yield function $I(E_p)$ is nonlinear, it is still single-valued and is known (or can be measured). The function $E_p(I)$ can be understood as the inverse, and the value of E_{p_i} can be calculated. Thus, the neutron energy can be expressed as

$$E_n = \sum_i (E_p(I_i)).$$

The pulse height response using such an approach will have a single peak, and the energy resolution will be determined primarily by the photoelectron statistics and will be significantly better.

2   Design of a Segmented Spectrometer

2.1   Principle of Design

To achieve the goal of compensating for the nonlinear light yield, it is necessary to distinguish the individual contributions from a common signal into separate recoil protons. Since neutron with an energy of a few MeV loses 90% of its energy within 10 ns in the scintillator, a time that is comparable to characteristic time of scintillation light, identification of these contributions using pulse shape of the signal from scintillator is practically impossible. To circumvent that problem, we divided the volume scintillator into optically independent segments, small enough that the probability of two scatters on hydrogen in one segment will be small (<10%). With such a partition, the majority of stopping neutrons create no more than one recoil proton in each segment. Using the amplitude of the signal from each photomultiplier tube (PMT), the energy of a recoil proton $E_p(I_i)$ in each hit segment is calculated, and summing E_{p_i}, one obtains the initial energy of the captured neutron. Note that more than 90% of the energy lost by a neutron occurs in the first few collisions with protons.

2.2   Individual Section Design

The pilot version of the spectrometer consists of 16 single segments. Each segment consists of a 3-cm diameter quartz tube with a 2-mm thick wall. The tubes are 15 cm in length with 1.2-cm quartz light guides glued at both ends of the tube. It is filled with 80 ml of

whitespirit-based scintillator with a light-yield about 40% of anthracene and a hydrogen-to-carbon ratio of ~1.8. In this pilot version of the detector, there is no ^{6}Li added to the scintillator. Instead of capture on ^{6}Li, a special mode of operation is used (and discussed below). The outer surface of each tube is carefully polished, so the light is collected at the ends is due to internal reflection. Each segment is viewed by two PMTs at the end of the tube. The PMTs are FEU-85 produced by the MELZ company (Moscow, Russia) and have 15% of quantum efficiency at 420 nm. Each PMT is supplied with high voltage produced by bases (cells) from the HV-System company (Dubna, Russia) [4]. The nonuniformity of light collection along the tube was measured to be within ±5%. In order to optically isolate the segments, each tube is wrapped with aluminized mylar.

2.3 Data Acquisition System

The design of the data acquisition system (DAQ) depends on the logic of neutron event selection in a background of γ-events. We consider a typical fast neutron event in the sectioned spectrometer with full deceleration in the scintillator and its capture on ^{6}Li.

PMT signals that are characteristic of proton recoil appear in sections simultaneously with a spread of less than 10 ns. Signals that are the result of slow neutron capture in the reaction $n + ^6\text{Li} \rightarrow \alpha + ^3\text{H} + 4.8$ MeV will occur later in a single section; the capture time depends on ^{6}Li concentration and is in the range (20–30) μs for our case. The amplitude of the signal is approximately 450 keV on the electron scale. The signals from both capture events and recoil events have large slow components and can be distinguished from each other and from γ-events by using of the pulse shape analysis (discrimination factor is ~10^3).

Thus, the neutron event in the sectioned spectrometer has an unique signature. The selection criteria of neutron events are 1) the number of triggered sections is greater than one; 2) the presence of two events in a time interval of 30 μs; 3) the slow component in the first and second signals corresponds to heavy particles; and 4) the amplitude of the second signal corresponds to energy release of a neutron capture on ^{6}Li. The joint application of these criteria allows one to achieve discrimination factor of >10^8 at γ-background of 10^2 s^{-1}.

The electronics and logic diagram that incorporates these criteria is shown in Figure 1. All channels function identically, and therefore one channel only is shown. The system is composed of commercial NIM and CAMAC equipment and a computer-based digital oscilloscope card. The PMT anode signals enter a low-noise mixer through matched 50-ohm coaxial cables. The impedance of the mixer inputs is 50-ohm DC, and its gain is unity. The output of the mixer enters the input of a fast buffer voltage amplifier with variable gain, which is necessary for gain matching the individual channels.

One output of the buffer amplifier enters a fast integral discriminator; the second output enters the input of a fast linear gate through a broadband coaxial 40 ns delay line in order to record of the initial slope of the waveform. The gate together with a delay line, discriminator, level translator (LT), and fast 16-channel mixer forms a linear multiplexer permitting a reduction in the electronic noise by a factor of $\sqrt{n}$, where n is the number of sections of the detector. The linear gate is controlled by a signal from a discriminator. Thus, the linear gate is open only when there is a control signal. The duration of the signal is 130 ns, corresponding to the pulse width and a time to compensate for the
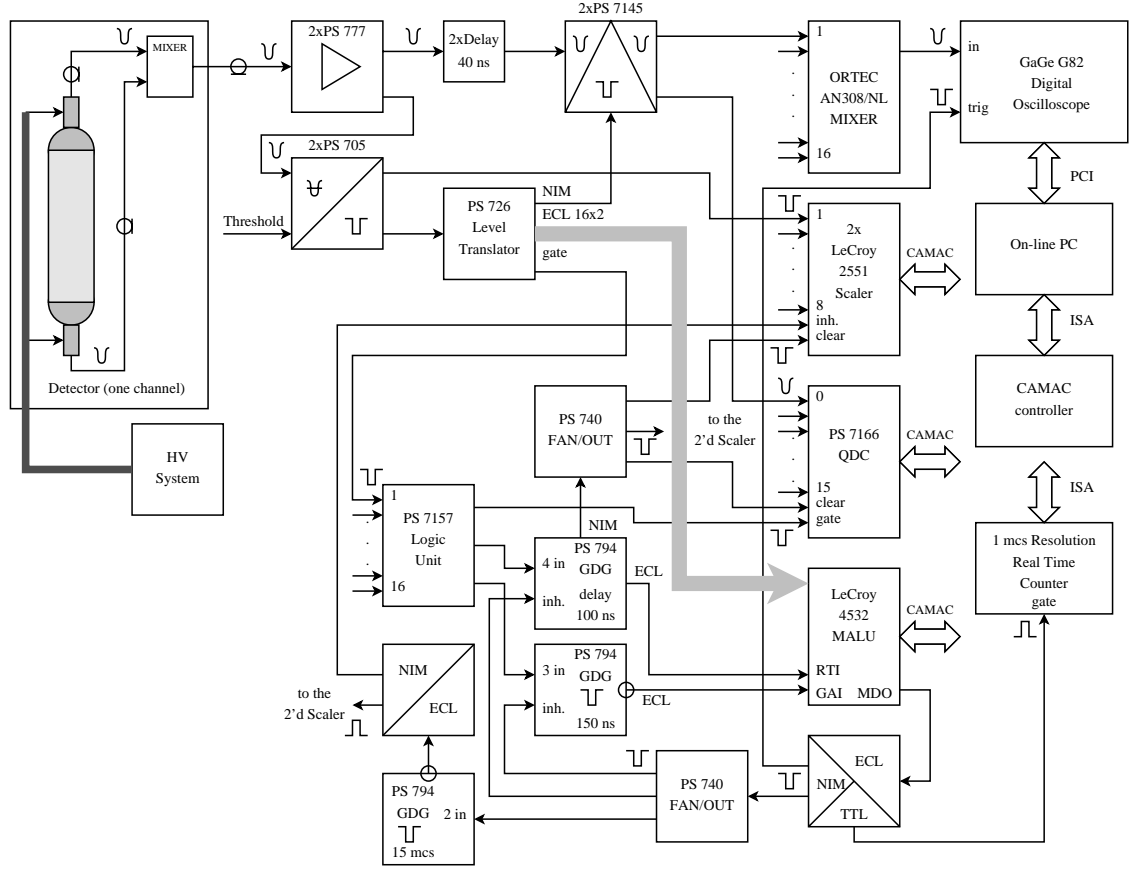
Figure 1: The functional diagram of the data acquisition system.

non-simultaneity of the signals from different sections.

From a linear gate, one output enters the input of the digital oscilloscope (DO) via a fast mixer, and a second output enters a multichannel integrating (charge-sensitive) QDC, which has 12-bit resolution. A conversion for all 16 channels in the QDC is produced by a gate signal from the OR operation of LT pulses in a logic unit.

The duration of the gate signal sets limits on the integration of the input signal. Of course, the duration of control signals for the linear gate and QDC are equal and exceed the duration of the PMT signals. The start of the DO is performed by the leading edge of a trigger produced by a MALU (Majority Logic Unit) from its MDO (Majority Discriminated Output) socket over an ECL/NIM level translator. The DO is set to a 32 kB frame size of the buffer memory; hence, a 1 ns of digitizing period corresponds to a time interval about 32 μs. In addition, another output of the discriminator enters a fast scaler, and paraphase pulses of ECL levels are input to the MALU unit. A real time counter with 1 μs resolution is used for precise system dead time measurement.

2.4   Acquisition Algorithm

In the initial state of the DAQ, operation of the scaler is inhibited by a logic 1 level, and the QDC is ready for conversion. The MALU, which operates in the memory enable mode, is already put in an open state by the logic 1 level on its gate input from the

inverted output of a gate and delay generator, which operates here as a NIM/ECL level translator for the trigger signal from the OR of a logic unit. The gate closes over a very short time interval, typically a few nanoseconds after accepting signals to its data inputs. This time interval is caused by the difference in cable delays. During the time when the gate is open, the internal register of the MALU collects signals from the appropriate inputs. After the gate closes, the data in this register are frozen, and an MDO level can be generated depending on the setting of the majority threshold M_{thr}. This threshold is adjustable and usually is set to a value greater than one for true neutron detection. The reset input of the MALU is controlled by the same trigger signal from the logic unit after being delayed by another gate and delay generator, which operates in the delay mode and uses the ECL output. The same signal from its NIM output enters to the clear inputs of the scaler and QDC through an active signal splitter module.

As a fast neutron decelerates in the scintillator, some number of discriminators corresponding to the detector sections will trigger simultaneously. For the detection of a gamma ray, however, typically one section will fire. PMT signals from triggered sections enter only the appropriate inputs of the QDC, and their sum is input to the DO. The QDC begins the conversion process immediately after the gate signal, thus latching the gate input.

In the case of γ-ray detection, the number of hits in the MALU register is one. An MDO level is not generated, and after 100 ns all the units (scaler, QDC and MALU) receive and external fast clear from a delayed trigger signal that is active at their appropriate inputs. The acquisition continues without software participation, and dead time is very small.

In the case of fast neutron detection, the number of hits in the MALU register is more than one. The MDO level is generated after a few tens of nanoseconds, starts the record at the DO, and inhibits the operation of the gate and delay generators, which is responsible for the generation of the reset and gate signals for the MALU and the generation the clear signal for the scaler and QDC. The third gate and delay starts with an MDO signal and enables operation of the scaler for $\simeq 30$ μs. If the slow neutron capture occurs during this interval, the scaler will increment one, which is one more selection criterion. The digitizing process at the QDC and the record at the DO will continue to the end. The acquisition software checks the LAM signal from the MALU, after which it waits for readiness of the QDC and DO, saves the data, and clears MDO output. Upon completion of the sequence, the system is reset to the initial state and acquisition continues. Obviously, the amplitude of all signals in the event, except for initial one, can be only defined by the record of the oscilloscope. This is not a problem because with the capture of a neutron, the correlation between the light yield and energy of the particles (^{3}H and ^{4}He) is unambiguous.

The DAQ system is ready for the full operation of the detector, but without ^{6}Li doped scintillator in the segments, the application of the DO is superfluous. In the current operation for fast neutron detection, the M_{thr} is set greater than one and the operation of the scaler is not inhibited. The total dead time of the acquisition is significantly lower in this mode.

2.5 Principle of Operation

There are two main modes of operation. First, in the case of $M_{thr} = 1$, the system is triggered by any hit segment, so one measures the scintillation in segments independently. The response of the detector looks like the response of an individual segment that is simply 80 ml of organic scintillator. Each section is designed so that both background γ-rays and neutrons of an intermediate energy range undergo, on average, a single scattering in a single segment. Thus, the response of the detector gives a Compton scattering distribution for monoenergetic γ-rays interaction and a flat step for monoenergetic neutrons. In the second mode, the system is triggered by three or more segments hit ($M_{thr} = 3$) within a few tens of nanoseconds. In this case the probability of the interaction being due to γ-rays is drastically decreased in comparison to that a fast neutron interaction. In addition, since the neutron loses on average about 90% of its initial energy after three collisions, it is a close approximation to the detector's operation when the scintillator is doped with ^{6}Li and requires the neutron capture. In this mode the neutron energy is obtained as a sum of recoil energies. Those energies are derived from the individual QDC values of each segment that fired and corrected by the electron-equivalent energy scale and the light-yield function. This is the main mode of operation for the pilot version of the detector for fast neutron measurements.

3 Response Function and Pulse Height Resolution

3.1 Calibration Sources

To measure the response of the detector on γ-rays, we used a ^{40}K source with a single 1.46 MeV line. The activity of the source was 10^3 Bq, and the distance between the detector and the source was 15 cm. The Compton edge of the line appears at 1.24 MeV, thus giving the electron equivalent energy scale.

The response to fast neutrons was measured with a Pu-α-Be source. It emits neutrons with a wide distribution of energies up to 10 MeV. In addition, 60% of neutron emission is accompanied by 4.44 MeV γ-rays (with a Compton edge at 4.2 MeV), so a sheet of 3-cm tungsten was used to shield the detector. The shield decreased the gamma intensity by a factor of 20 but does not distort the neutron spectrum significantly. The neutron emission rate of the source was 10^7 s^{-1}, and the distance between the detector and source was 80 cm.

The response function of the detector was measured using monoenergetic 14.1 MeV neutrons from a D-T source (commercial model UNG-1, Russia). Its principle of operation is based on fusion reaction ^{3}H(d,n)^{4}He. The emission rate of source was about 10^3 s^{-1}, the distances were $\simeq$0.2 m from the source to the detector and $\simeq$1 m to the wall of room.

3.2 Pu-α-Be source: Response and Resolution

Irradiation of the detector in $M_{thr} = 1$ mode by the ^{40}K γ-source shows a clear Compton edge at 1.24 MeV (see Figure 2) at approximately channel 700 of the QDC. The resolution

of the step is estimated to be (10–15)% and is a result of the dispersion in the response of an individual segment and the photoelectron statistics.
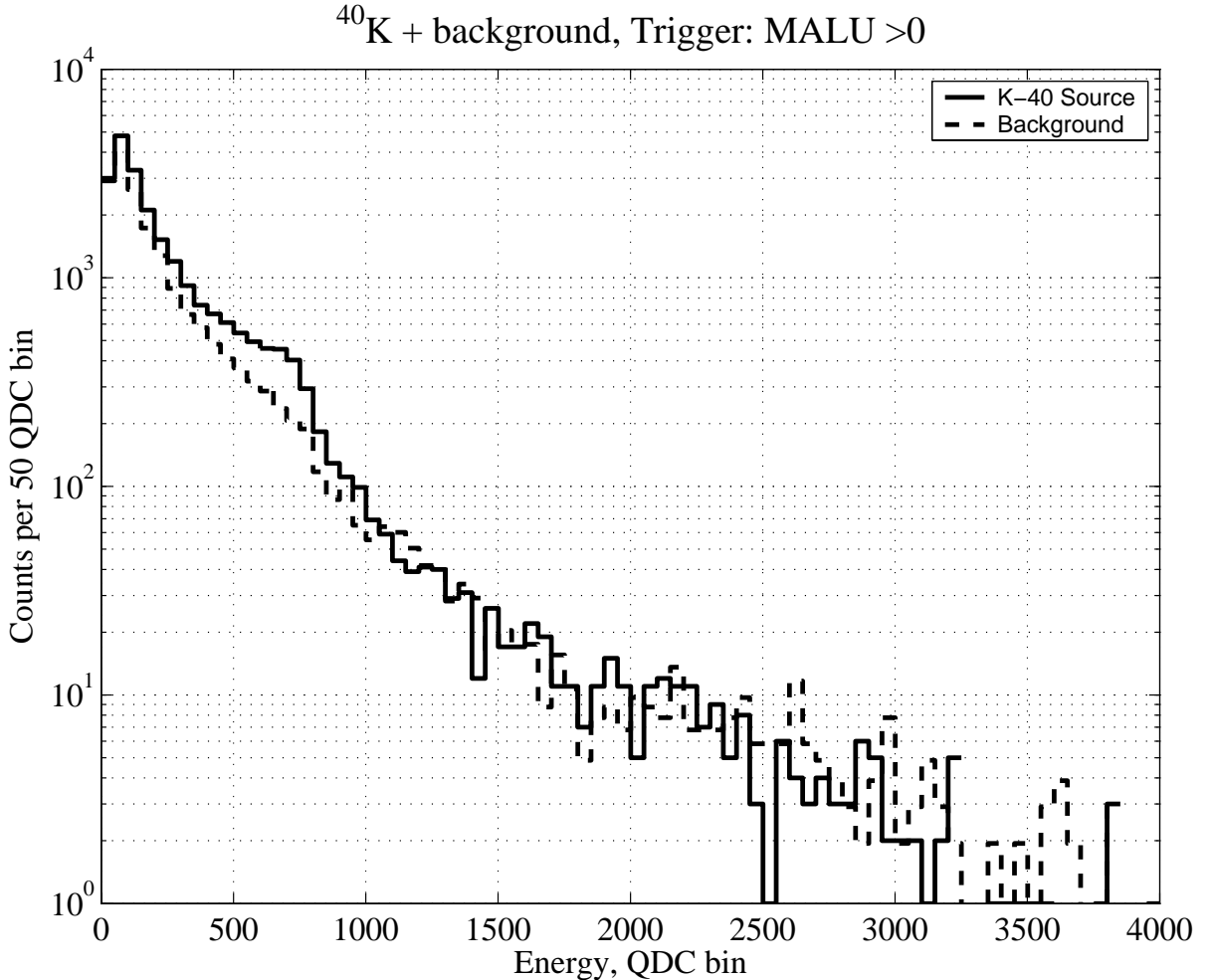

Figure 2: Detector response to 1.46 MeV γ-rays. The response is a sum of 16 individual responses from each segment.

When irradiated with Pu-α-Be source in the same mode without the shield, the response reveals a weak Compton edge of 4.44 MeV γ-rays also. In Figure 3 ones sees a small excess in the proper 4.2 MeV location (upper curve) in comparison with shielded response (middle curve). Another feature of the response is a threshold of individual segments for recoil protons. It occurs around 100 keV in the electron-equivalent energy scale, corresponding to 600 keV of recoil energy.

In the mode of $M_{thr} = 3$, there is essentially no evidence of a ^{40}K γ-source. When irradiated with the Pu-α-Be source, the neutron energy is obtained as the sum of the recoil energies derived from the individual QDC value of each hit segment. Without the tungsten shielding, occasionally a random coincidence can occur from one segment hit by the 4.44 MeV γ-ray and two segments hit by a single neutron. The QDC value of the segment hit by the γ-rays obviously distorts the final neutron energy. This is why the response of the unshielded source looks flat in the energy range of 2 MeV to 8 MeV,
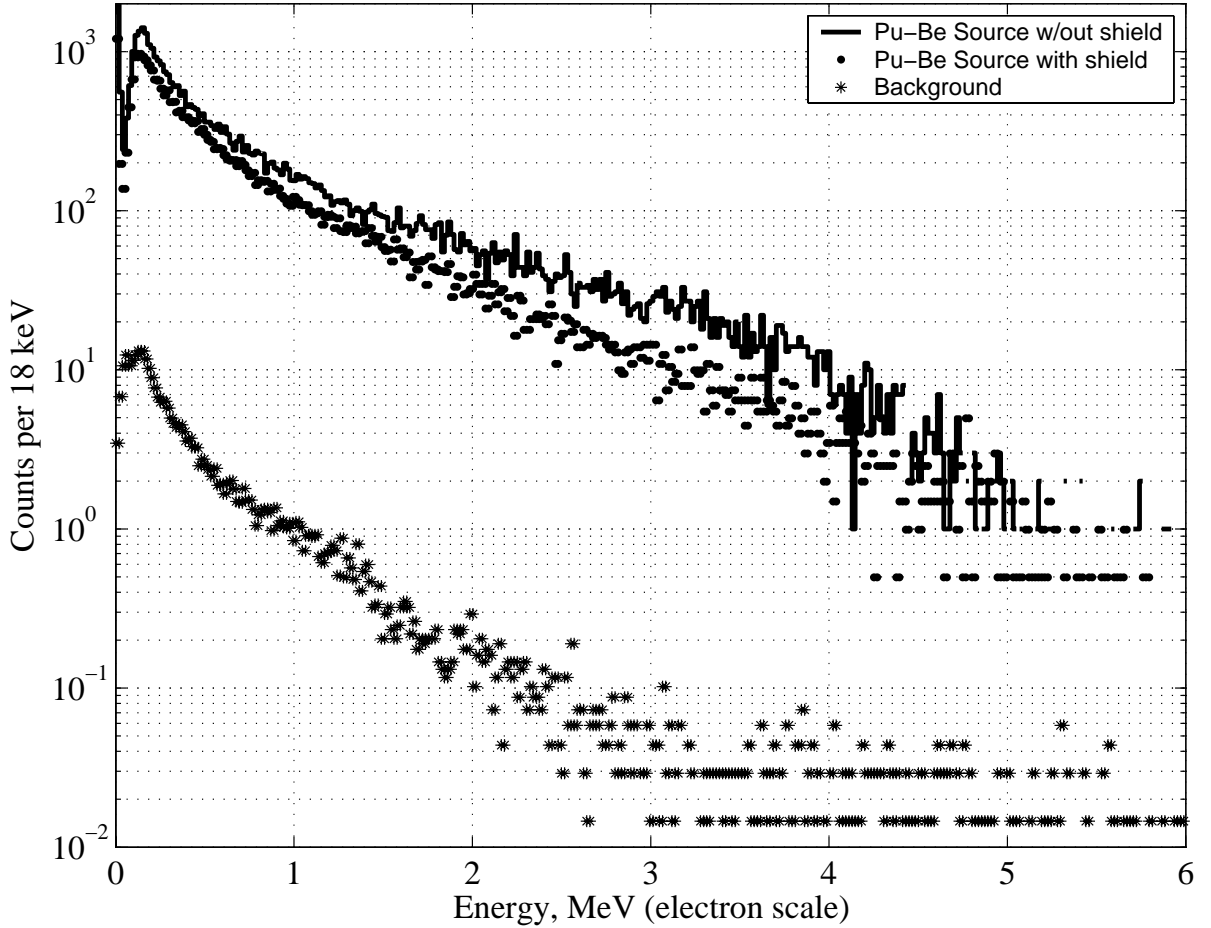
Figure 3: Detector response to a Pu-α-Be source, $M_{thr} = 1$.

as seen in the upper curve of Figure 4. The tungsten shielding strongly suppresses the contribution of the accompanying γ-rays, and one can see the undiluted response to neutrons (middle curve).

The effective neutron threshold in the $M_{thr} = 3$ mode differs from that of 600 keV in the $M_{thr} = 1$ mode. The minimal neutron energy that can be detected is 3×600 keV = 1.8 MeV. The probability that the energy will be uniformly distributed among three recoils is rather small. It is much more probable to encounter, for example, recoils with energies of 600 keV, 1200 keV, and 2400 keV producing 4.2 MeV of neutron energy. Hence, one would expect that an effective neutron threshold should exist somewhere in the middle of those values. The measured response in Figure 4 indicates that the threshold lies around 3 MeV, which is in agreement with this consideration.
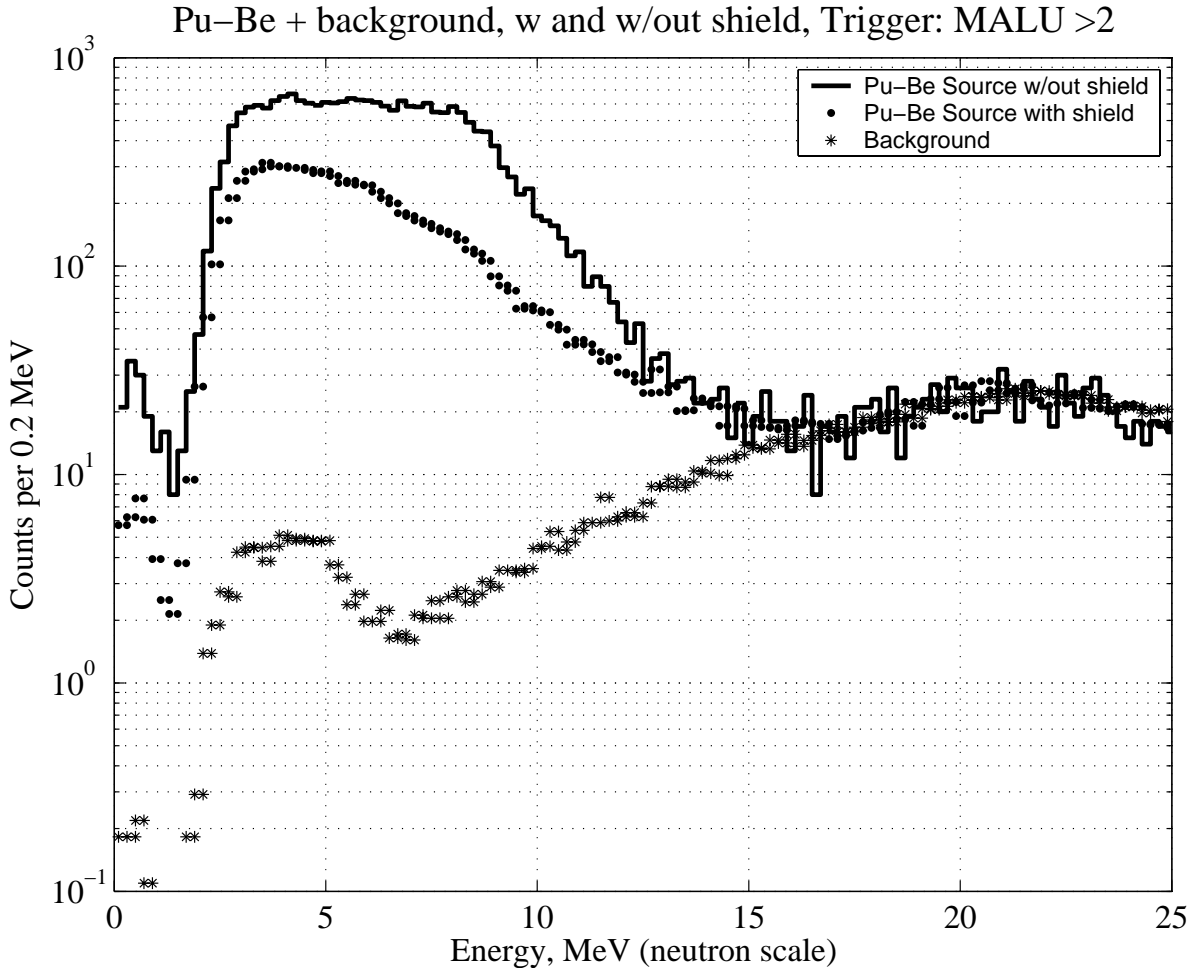
Figure 4: Detector response to a Pu-α-Be source, $M_{thr} = 3$.

3.3   14.1 MeV neutrons source: the Response Function measurement

There were made four measurements. Their statistical data are shown in Table 1, where Run — data file number, M_{thr} — MALU threshold, Thr — hardware threshold, N_{ev} — number of events in the run, Rate — average rate of events in the run and $Rate_{sc}$ — summary scaler rate for all sections. The details of the measurements are described below.

First, we measured response of single sections ($M_{thr} = 1$) that gave us the energy scale. Before the measurements we decreased the gain to set the step in 3/4 of full QDC scale and increased the hardware threshold at five times to record the step in more detail. The middle of the step appears at 2900 QDC bin (Figure 5), and it corresponds to 8.0 MeV of electron energy scale due to light-yield curve, which is given in [5] and can be expressed as (1):

$$E_{ee} = 0.95\, E_{p} - 8.0\left[1 - \exp(-0.1 E_{p}^{0.9})\right], \tag{1}$$

where E_{ee} and E_{p} are in MeV for energies of electrons and protons accordingly. This

Table 1: Response Function measurement: statistical data

Run	M_{thr}, hits	Source, MeV	Thr, mV	Live Time, s	N_{ev}	Rate, s^{-1}	$Rate_{sc}$, s^{-1}
094303	1	-	100	1157	27215	23.5	30
101459	1	14.1	100	167	89835	538	542
104231	3	14.1	20	2481	11305	4.6	865
114105	3	–	20	9260	18676	2.0	114

equation yields negative light yield for $E_p < 0.2$ MeV, but it is not a problem in our case because a 20 mV threshold for individual segments corresponds to 0.8–1.0 MeV of recoil energy.
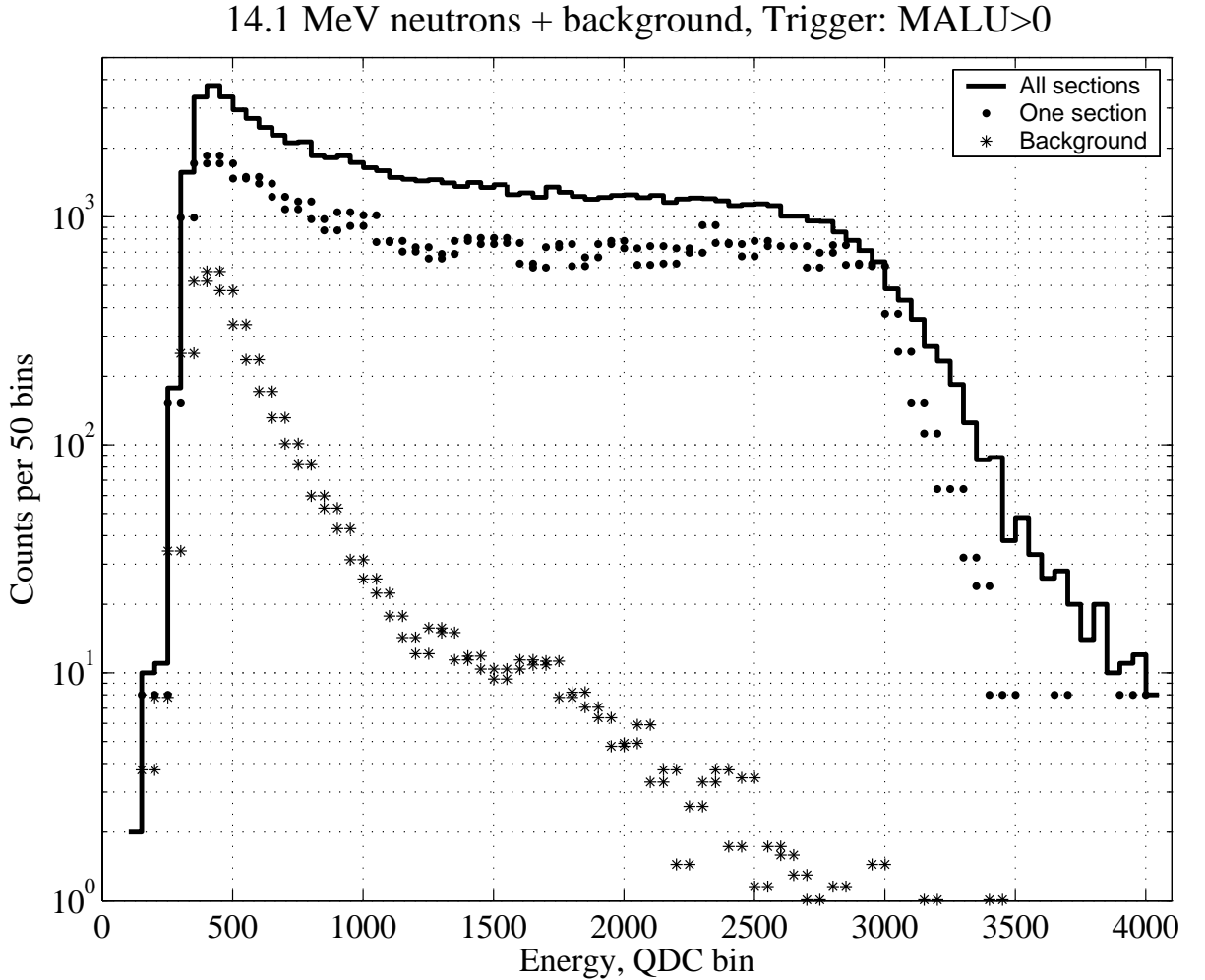

Figure 5: Step response for 14.1 MeV neutrons. $M_{thr} = 1$

The resolution of the step is mainly due to dispersion of each PMT, which is follows from comparison of the step responses from all sixteen sections and the single section of

the detector in Figure 5. The main reason of dispersion is obviously that they are not proper glued to lightguides. Another reason is that HV-cells have poor resolution in set values.

Second, we measured the pulse height response of the detector on 14.1 MeV neutrons with $M_{thr} = 3$. It appeared to be like clear peak even on wide muon background distribution (Figure 6). With application of the correction curve for energy determination of recoil protons, which was obtained according to procedure described in Section 1, we have got the response at neutron energy scale.
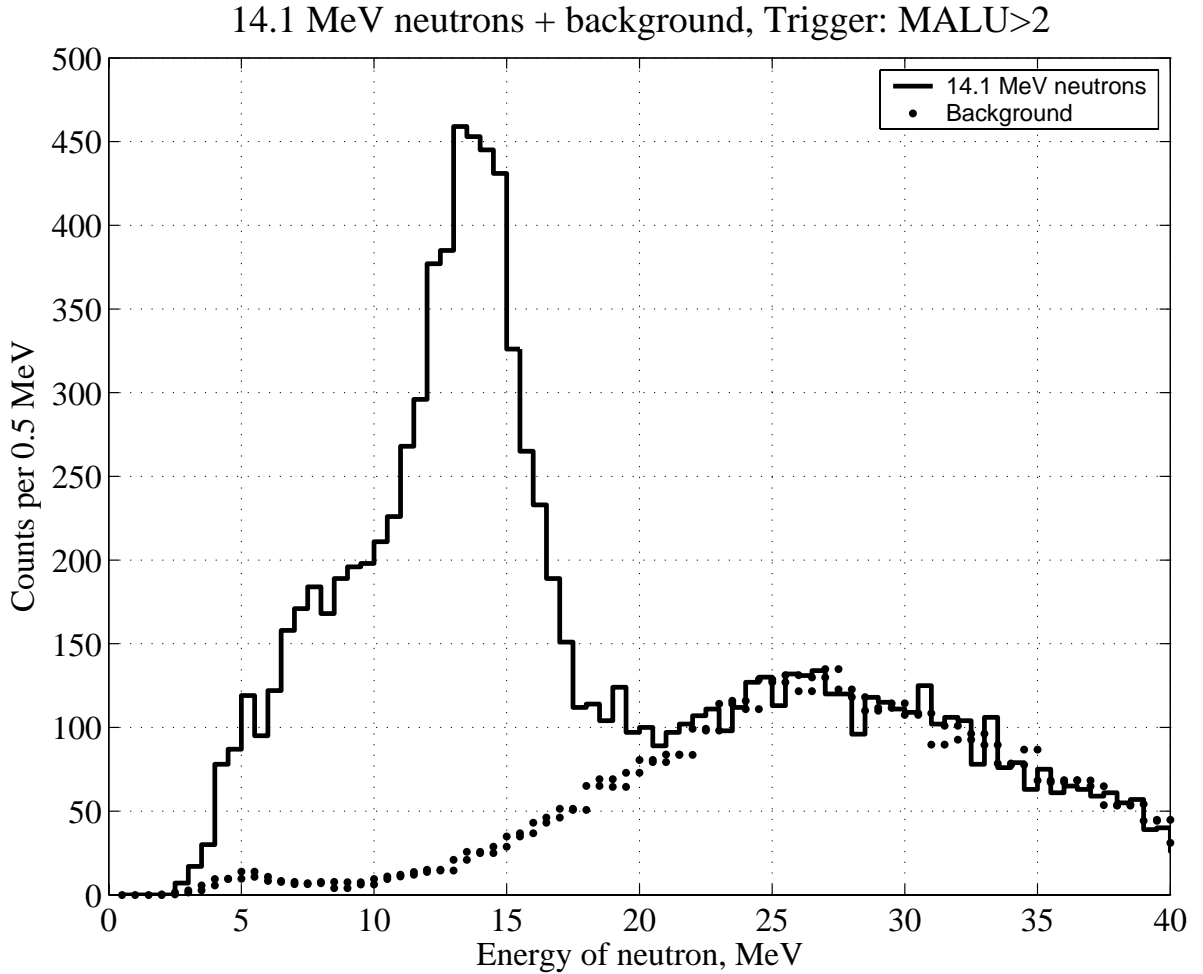

Figure 6: 14.1 MeV neutrons energy distribution on cosmic muons background

Clear distribution of cosmic muon background was obtained at the measurement with same conditions, but without neutron irradiation of the detector. It is shown in Figure 6 by the bold dots.

The pulse height resolution looks rather poor (FWHM $\simeq 30\%$), but definitely it can be greatly improved. The effective neutron threshold is 3 MeV, which corresponds to our estimations for these conditions.

4   Conclusions

The first test of the pilot version of the segmented fast neutron spectrometer has demonstrated that it operates in accordance with expectations. Its response to neutrons over a broad energy range shows no unexpected behavior. The response function of the detector on 14.1 MeV neutrons from D-T fusion is obtained and is presented at first time. The measured pulse height resolution is about 30%. One of the reasons for the relatively poor resolution is the absence of ^{6}Li as an effective capture material.

The effective neutron threshold is about 3 MeV. There are several things which determine the threshold. First, it is obviously an apparatus threshold of single section. Right now it is 20 mV and it corresponds to 0.8–1.0 MeV of recoil energy. It can be easily decreased twice but it requires some improvement in discriminator module. Now it looks to be not so stable and at low level signals with noise it may produce several consequent gates. Second, an improved PMT and HV-cell combination as well as an improved segment design will allow one to make the sections much more uniform. It will improve the resolution of the step (and pulse height resolution of the detector response function also) and as a result will allow one to put the middle of step in 4/5 of QDC full scale (instead of 3/4 now). Obviously it will decrease threshold. Another reason here is the noise of PMT — now it looks not so good. Last, one should remember that the threshold of single section is not direct threshold just because of that a normal MALU threshold is now 3 or more hits. It increases the effective threshold according to average lose of 1/2 of intitial neutron energy in each collision up to 3–4 MeV that we see at real spectrum. Thus, introducing ^{6}Li or other capturer in the detector we may trigger with 2 or even 1 hits, drastically decreasing the effective threshold.

Acknowledgments

References

[1] Kamykowski *et al*, NIM A 317 (1992) 559.

[2] Aoyama *et al*, NIM A 333 (1993) 492.

[3] Abdurashitov *et al*, NIM A 476 (2002) 318.

[4] Mailto: astakhov@sunhe.jinr.ru

[5] Scintillators for the physical sciences. Brochure No. 126P, Nuclear Enterprises Inc., Feb. 1980.